Hindawi
Advances in Civil Engineering
Volume 2022, Article ID 9552620, 12 pages
https://doi.org/10.1155/2022/9552620

Research Article

Coal and Gas Comining in the High-Gas Detong Mine, China: Analytical and Numerical Parameter Optimization of Gas Extraction Boreholes

Wei Wang,[1,2] **Zongxiang Li**,[1] **Guangmin Zhao**,[2] **and Yujin Chen**[3]

[1]*College of Safety Science and Engineering, Liaoning Technical University, Liaoning, 123000, China*
[2]*Division of Energy, Shuifa Group Co., Ltd, Jinan 25000, China*
[3]*Shuifa Zhongxing Group Co., Ltd, Jinan 25000, China*

Correspondence should be addressed to Zongxiang Li; lzx6211@126.com

Received 2 December 2021; Accepted 4 February 2022; Published 4 March 2022

Academic Editor: Gaofeng Song

The upper corner gas overrun caused by goaf gas gushing in the high-gas mine can be mitigated by roof positioning of long boreholes in the goaf fracture zone, creating an artificial gas migration channel and achieving safe comining of coal and gas. This study numerically simulated the fracture evolution in the coal rock overlying goaf in workface #2-104 of the Detong Mine, China. Using the O-shaped circle theory and the FLAC^{3D} commercial software package, the range parameters of goaf fracture zone gas-concentrated areas were obtained by defining the pressure relief coefficient, which provided a basis for the arrangement of holes in the goaf located at 15 m from the workface goaf collapse zone to the workface floor and 15–60 m from the structure zone to the workface. According to the obtained goaf parameters, the distribution and migration law in the goaf under the conditions of initial state and extraction with different roof borehole parameters were simulated by the FLUENT software. The optimal borehole location was 30 m from the floor and 25 m from the return airway. The field experiment with three boreholes arranged in the optimal extraction position provided the extraction concentration in the borehole above 30%, the gas extraction volume of 12 $m^3 \cdot min^{-1}$, and the concentration at the upper corner below 1%, which ensured safe coal and gas comining.

1. Introduction

While coal mining intensity and depth keep growing annually with increased coal demand, mine productivity is restricted by gas outburst risks. Since mining gas is also a clean energy resource, the realization of coal and gas comining is conducive to improving the utilization rate of resources and reducing greenhouse gas emissions [1]. Influenced by the mining and overburden, the fracture zone generated by the bending and separation of the goaf roof becomes a high-concentration gas area, which is the key area to control goaf gas and prevent the overrun of the upper corner gas of the mining face [2]. A recent theoretical study comprehensively integrated the O-shaped circle theory, pressure relief mining and pumping, and coal and gas comining [3]. Based on the subsidence of a coal mine in Britain, Fang et al. [4] reported that the compaction and stress recovery of rock mass in goaf were mainly related to mining height, buried depth, and other parameters. They performed the numerical regression analysis of the goaf compaction mechanical properties via the FLAC^{3D} software. Cheng et al. [5] concluded that the mining fracture of the overburden had the characteristics of ∩-shaped high cap. Qian and Xu [6] revealed a circular fault zone developed above the goaf, constituting a gas accumulation zone and migration channel. Yavuz [7] analyzed the elliptical paraboloid zone's pressure relief gas extraction mechanism and proposed the corresponding coal and methane comining technology. Karacan et al. [8] investigated the effect of the coal mining fracture field on mining stress distribution and coal seam gas pressure. Guo et al [9] coupled the permeability field with the results of the mechanical model and

proposed a comprehensive "dynamic" gas reservoir model to simulate the effect of gas gushing and extraction on goaf gas production. Li et al. [10] analyzed the evolution and development law of the goaf gas macroflow channel based on the scale and time effect of the rock mass. Although the above studies provide a theoretical basis for gas accumulation in the goaf and the realization of coal and gas comining, no practical control measures have been proposed. The method proposed in Li et al. [10] can solve the problem of gas accumulation and lacks operability in practical applications. According to the evolution of goaf overburden fracture under mining, the extraction height of roof HLB and its optimal extraction parameters were determined through numerical simulation.

2. Fracture Development of Overburden and Gas Accumulation in the Upper Corner in Goaf

After mining the coal seam, the coal rock mass accumulates in goaf. According to the evolution of coal rock mass, accumulation state, and gas flow characteristics, the mining space can be subdivided into collapse zone, fracture zone, and bending subsidence zone [11]. The coal seam mining reduces the goaf support, triggering numerous secondary fractures in the collapse and fracture zones, which turn into the main migration channel for the gas. With the workface advance, macrocracks developed in the overburden in the middle of goaf are gradually compacted and closed by the ground pressure. The porosity in goaf exhibits nonuniform and continuous distribution patterns, resulting in an O-shaped structure zone [12]. The gas in goaf floats up and accumulates in the O-shaped structure zone due to the buoyancy, forming gas concentration areas. The schematic diagram of the three-band distribution has been shown in Figure 1. Due to goaf air leakage, gas flows into the upper corner, resulting in gas overrun [13].

Under U-shaped ventilation conditions, the air flow in the goaf flows from the transportation lane of the working face to the cut-off hole of the working face, a small part of which flows to the goaf, and most of the working face flows. The air leakage in the goaf presents a parabolic shape, which brings out the gas in the deep part of the goaf, where the upper corners of the working surface meet, so that the upper corner of the working surface has a higher gas concentration. At the same time, because the upper corner of the coal mining face is close to the coal wall and the goaf, when the wind flow passes the end of the working face, the wind speed near the coal wall is reduced due to the sudden vertical turn of the roadway, and vortex phenomenon appears in the upper corner of the working face. There is a phenomenon of air circulation in the vicinity, so that the gas in the goaf and working face is not easily taken away by the wind, and the gas in the upper corner is prone to accumulate.

Therefore, besides controlling the air leakage in goaf, one has to provide the goaf gas control and upper corner gas overrun prevention. To this end, a continuous artificial negative pressure channel should be set in the gas concentration area in the fracture zone, overlying the goaf to drain the gas in goaf by the pressure gradient to prevent gushing out of high-concentration gas.

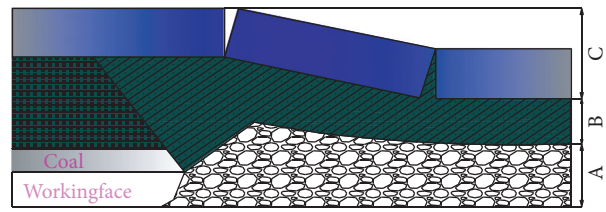

(A) Collapse zone
(B) Fracture zone
(C) Bending subsidence zone

Figure 1: Distributions of three fracture development zones of overburden in the goaf. (A) Collapse zone. (B) Fracture zone. (C) Bending subsidence zone.

3. Determination of the High-Efficiency Pumping Area of Goaf Gas

3.1. Evolution of Goaf Overburden Simulated by FLAC^{3D}. To investigate the evolution of overburden in goaf after coal seam mining and determine the optimal position of roof HLB, this study used the FLAC^{3D} software package for simulating the plastic stress variation and distribution of overburden after coal seam mining, which provided a basis for studying goaf gas movement law and determining the optimal extraction parameters.

Detong Coal Mine is located in Linfen City, Shanxi Province, and the mine field is located in the north of Hedong Coal Field, the coal mining method of the working face has adopted the strike longwall mining method, the average thickness of the coal seam is 5 m, the mining height is 4 m, and the coal seam is buried at a depth of about 390 m. The "U" type ventilation method is used and the roof lithology is sandy mudstone and mudstone, and the floor lithology is mudstone and sandy mudstone. Based on workface 20104 of the Detong Mine, distance a model with a length of 430 m, a width of 295 m, and a height of 382.3 m was established in this paper. According to the field measurement results, the model's vertical and horizontal stresses (σ_z and σ_x) were 20 and 18 MPa, respectively. The main mechanical parameters of numerical simulation were obtained based on the geological data and geological histogram. The Mohr–Coulomb criterion was adopted for stresses in the simulation [14]. The particular strata of the coal rock mass are described in Table 1, and the established model is shown in Figure 2(a).

The length of a unit square in Figure 2 in the direction of the coal seam advance was 5 m. When the excavation length reached 120 m, the plastic failure area continued to expand along the advancement direction but remained stable and unchanged in the vertical direction. The range of the plastic failure area was 60 m from the floor, and its upper limit could be considered the upper bound of the fracture zone [15], which was consistent with the calculation results. Thus,

Table 1: Physical and mechanical properties of rock strata.

Stratum	Buried depth, m	Thickness, m	Density, kg·m^{-3}	Bulk modulus, GPa	Shear modulus, GPa	Internal friction angle	Cohesion, MPa	Tensile strength, MPa
Argillaceous sandstone	0	100	2790	8.6	4.65	34	4.31	1.8
Coarse sandstone	−100	178	2860	2.9	2.5	32	2.1	2.1
Siltstone	−278	54	2540	5.38	2.74	35	2.23	0.6
Medium grained sandstone	−332	35	2650	7.2	3.53	35	3.26	2
Conglomerate rock	−367	10	2610	4.55	2.58	32	2	2.4
Coal	−377	5.3	1400	1.19	0.37	23	0.8	0.5
Siltstone	−382.3	3.4	2580	5.61	2.35	36	2.15	0.7

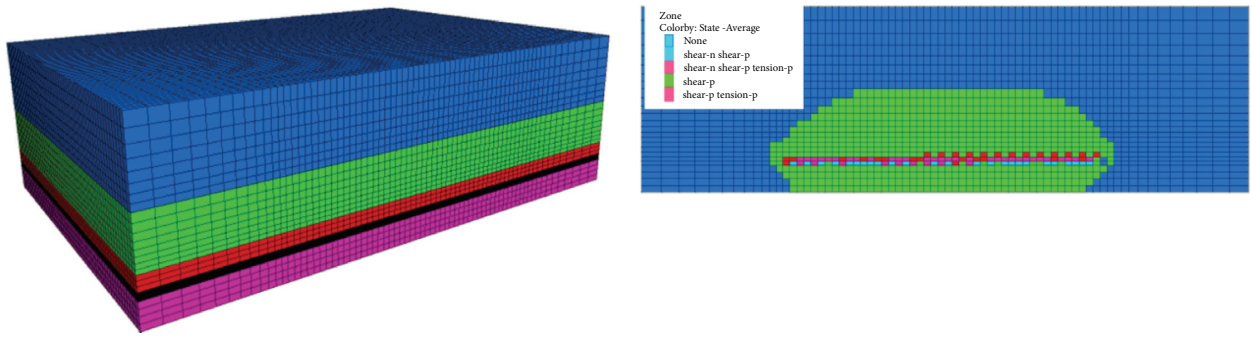

(a) (b)

Figure 2: Numerical calculation model (a) and stress state distribution map (b) of the goaf.

it could be concluded that the upper limit of the fracture zone was 60 m.

The goaf collapse zone could be determined according to the value and direction of the maximum and minimum horizontal principal stresses σ_H and σ_h after mining. At $\sigma_H > 0$ and $\sigma_h > 0$, it was a bidirectional tensile stress zone mainly distributed in the goaf collapse zone rock mass [15].

In this way, the distributions of the maximum and minimum horizontal principal stresses were obtained through FLAC^{3D} numerical simulation, as shown in Figure 3.

According to the simulation results, coal seam mining led to stress redistribution in the surrounding rock mass. In the process of stress balancing, a series of mechanical effects such as overburden caving, collapse, separation, and displacement of the overlying coal seam strongly manifested themselves. With the workface advance, the goaf behind the workface was gradually compacted under the overburden weight. As observed, the goaf caving zone was mainly distributed within 15 m from the floor , so the distance from the collapse zone to the floor in further calculations was taken as 15 m.

3.2. Distribution of Gas Infiltration Zone in Goaf Undermining. In the process of gas adsorption-desorption dynamic equilibrium, if the gas is in a saturated adsorption state, the adsorbed gas will be desorbed as the coal body is unloaded; if the gas is in an unsaturated adsorption state, the coal body needs to reach a certain value when the pressure is relieved. The pore gas pressure is reduced to the critical gas desorption pressure and the gas is desorbed. This pressure relief value can be called the effective pressure relief coefficient for gas desorption and drainage. In other words, the lower the saturation of gas adsorption, the higher the degree of pressure relief required for large-scale gas desorption. To observe the coal rock mass evolution after coal seam excavation, the pressure relief coefficient r was defined as

$$\gamma = 1 - \frac{\sigma_Z}{\sigma_0}, \tag{1}$$

where σ_Z is the vertical pressure after coal seam excavation and σ_0 is the initial pressure.

A previous study [16] revealed that the effective extraction range of gas required a great pressure relief degree of coal rock. Based on the research results, the effective pressure relief coefficient can be preset at 0.8 (i.e., $\sigma_z = 0.2\sigma_0$), which corresponds to the efficient extraction range. The numerical simulation performed via FLAC^{3D} software predicted the distribution of workface vertical pressure. The simulation results were sliced according to the distribution range of the collapse and fracture zones, yielding the stress distributions in goaf at different heights, as shown in Figure 4.

According to the pressure relief distribution of the vertical slice, the O-shaped compaction stress rising area was observed in the overlying strata of the workface, and a "vertical stress relief ring" was observed near the O-shaped

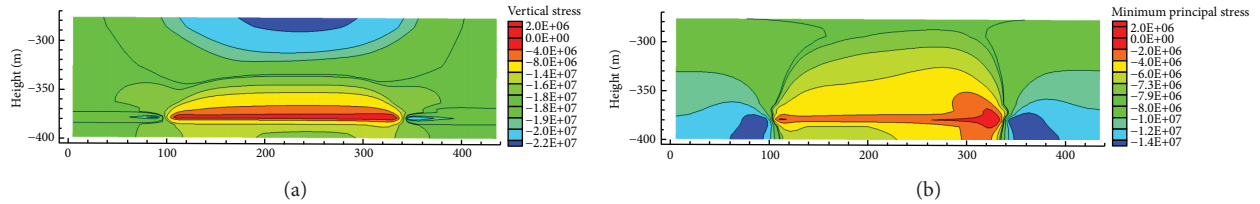

Figure 3: Distributions of the maximum (a) and minimum (b) principal stresses in goaf along the strike direction.

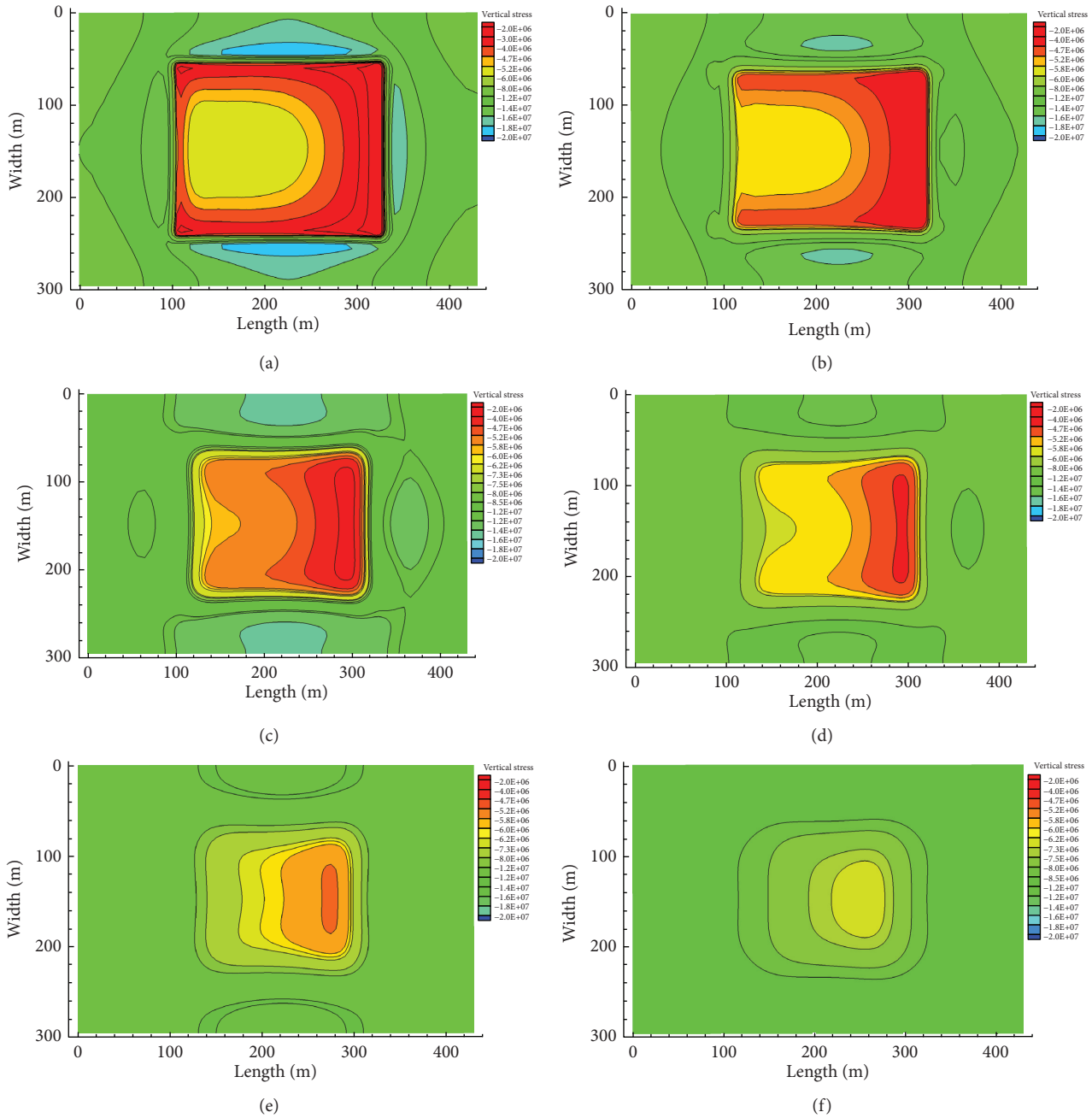

Figure 4: Vertical stress distribution at various horizontal distances from the floor: (a) 0 m; (b) 10 m; (c) 30 m; (d) 45 m; (e) 60 m; (f) 75 m.

compaction stress rising area. With an increase in the slice height, the stress in the pressure relief area of the overburden increased gradually and returned to the initial rock stress value; the stress variation rate in the surrounding rock gradually decreased, which was in line with the O-shaped circle theory [3]. As observed, a large pressure relief area was observed near the back of the workface. With an increase in goaf height, the range of the pressure relief area gradually reduced, and this area should be avoided in the extraction drilling arrangement to prevent the borehole cut-off, which would deteriorate the gas extraction efficiency.

The simulation results revealed that the area with an initial vertical pressure of 20 MPa and pressure relief coefficient of 0.8 was within the range of 0–45 m from the floor height. To avoid the drilling being cut off, the drilling should avoid the area with the pressure relief coefficient >0.8. The optimal height range of the pressure relief channel was 15–45 m. According to the distribution range of pressure relief coefficient and trigonometric function, the effective pressure relief angle of gas efficient extraction range was 76° in the strike and 85° in the dip directions. The area with a pressure relief coefficient of 0.2 was a low-permeability gas area, which could be used as a compaction area. According to the simulation results, the distance between the boundary of the compaction area and the workface was 20 m.

4. Gas Migration Law in Goaf Pressure Relief Area

The migration of gas mixture in goaf was comprehensively affected by air leakage, emission amount of workface gas, and the pressure of coal rock mass in goaf. A further numerical simulation was performed for the case study of workface #2-104 of the Detong Mine, China.

4.1. Goaf Gas Migration Control Equation and Assumptions. For the convenience of calculation, the go extraction area (goaf) was simplified as follows:

(1) The influence of shearer, hydraulic prop, and electromechanical equipment on the fluid in coal mining workface was ignored

(2) The mining workface, intake airway, return airway, and goaf areas were assumed to be cuboids, and the gas was treated as an incompressible ideal gas

(3) The goaf was assumed to be porous and isotropic [17]

(4) The gas flow was regarded as isothermal motion, and the influence of water vapor and other gases in goaf was ignored

According to the above assumptions, the goaf can be geometrically modeled and meshed, as shown in Figure 5.

According to the above assumptions, the gas mixture flow in goaf satisfied the mass and momentum equations [18].

The fluid flow in the goaf followed Darcy's law, which could be expressed as

$$s_i = -\frac{\mu}{\alpha}\nu_j, \tag{2}$$

where s_i is the source term of the i^{th} momentum equation; μ is the viscous resistance coefficient, *Pa·s*; α is the permeability coefficient of porous media, m^2; ν_j is the velocity component.

The flow model that could deal with the turbulent state of gas flow was $k-\varepsilon$ turbulent model, derived by a rigorous statistical technique, and the equations of turbulent kinetic energy k and dissipation rate ε were as follows [19]:

$$\begin{aligned}
\frac{\partial(\rho k)}{\partial t} + \frac{\partial(\rho\mu_i k)}{\partial x_i} &= \frac{\partial\left[\left(\mu + \left(\mu_t/\sigma_k\right)\right)\left(\partial k/\partial x_j\right)\right]}{\partial x_j} + G_k + G_b - \rho\varepsilon - Y_M + S_k,\\
\frac{\partial(\rho\varepsilon)}{\partial t} + \frac{\partial(\rho\mu_i\varepsilon)}{\partial x_i} &= \frac{\partial\left[\left(\mu + \left(\mu_t/\sigma_\varepsilon\right)\right)\left(\partial k/\partial x_j\right)\right]}{\partial x_j} + C_{1\varepsilon}\times\frac{\varepsilon}{k}\left(G_k + C_{3\varepsilon}G_b\right) - G_b - C_{2\varepsilon}\rho\frac{\varepsilon^2}{k} + S_\varepsilon,
\end{aligned} \tag{3}$$

where μ_t is the turbulent viscosity, μ_i is the average velocity, ρ is the density, G_k is the turbulent kinetic energy generation term caused by velocity gradient, S_ε/S_k are the custom source terms, and $C_{1\varepsilon}/C_{2\varepsilon}/C_{3\varepsilon}$ are the empirical coefficients.

4.2. Gas Sources in Goaf Analysis and Calculation. The gas sources of goaf mainly included the gas gushing out of workface (q_1), of adjacent layer (q_2), and out of goaf (q_3). Under the action of buoyancy and air leakage, part of the gas gushed out with airflow, and the other part floated up and was stored into the cracks induced by mining.

These processes are expressed as follows [20]:

$$\begin{aligned}
q_1 &= \lambda\cdot\frac{m}{H}\left(W_0 - W_c\right),\\
q_2 &= \sum_{i=1}^{n}\left(W_{0i} - W_{ci}\right)\cdot\frac{m_i}{H},\\
q_3 &= l\cdot q_0\cdot\nu_0\left[\exp\left(-\sqrt{\frac{l_1}{\nu_0 t}}\right) + \exp\left(-\sqrt{\frac{l_2}{\nu_0 t}}\right)\right],
\end{aligned} \tag{4}$$

where q_1 is the amount of gas gushing from the mining layer, q_2 is the amount of gas gushing from the adjacent layer, q_3 is the amount of gas gushing from the residual coal in the goaf, λ is the gas gushing coefficient, W_0 and W_c are the initial and

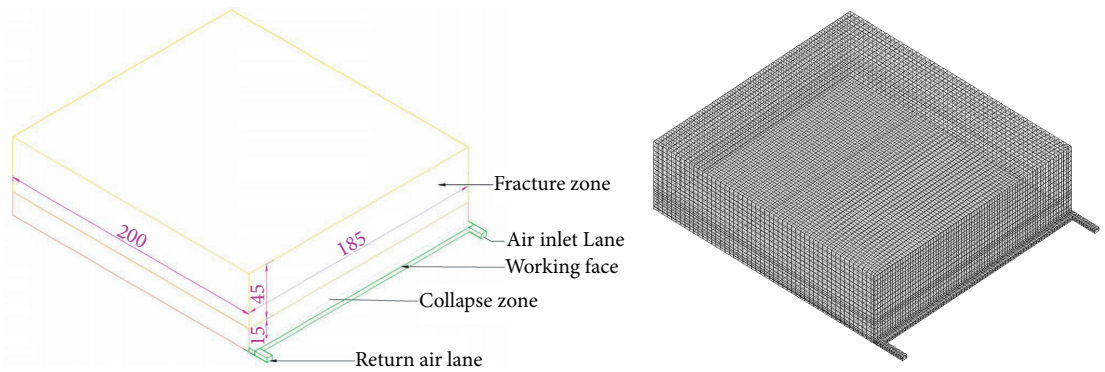

Figure 5: Numerical simulation model. (a) Geometric model of working face. (b) Mesh generation of working face.

residual gas contents, respectively, m is the mining layer thickness, i is the parameter of the i^{th} adjacent coal seam, V_0 is the mining velocity of workface, t is the coal seam exposure time, l is the perimeter of roadway section, l_1 is the workface length, l_2 is the strike length of goaf, and q_0 is the gas gushing intensity of the coal wall.

4.3. CFD Numerical Simulation of Mixture Gas Flow in Goaf. The parameter values of each calculation formula shown in Table 2 were obtained based on the field measured data and the empirical formula.

Therefore, parameters q_1, q_1, and q_3 were taken as 2.97×10^{-5}, 1.85×10^{-9}, and 2.6×10^{-8} kg·(m^3·s)$^{-1}$, respectively.

4.3.1. Geometric Model. According to the actual dimensions of the site and used scale, the geometric model was set as follows:

(1) The coal mining face's length, width, and height dimensions were $185\times5\times4$ m, and the space type was fluid

(2) The scale of the intake and return airway was $10\times4\times4$ m, and the space type was fluid

(3) The scale of goaf was $185\times200\times60$ m, the fracture and collapse zones were 45 and15 m from the floor, respectively, and the space type was porous media

4.3.2. Boundary Conditions. The return airway was set as "Out-flow" in the simulations, while the intake airway was assigned a "Velocity-in" value of 2.5 m·s^{-1}.

Since the goaf was regarded as porous media, its permeability was required for calculations. Therefore, the following permeability model based on sigmoid function was used to simulate the permeability parameter evolution [21].

$$\kappa = \kappa_{\min} + \frac{\kappa_z}{1+e^{\alpha_1 x-5}} + \frac{\kappa_z}{\left(1+e^{\alpha_2 x-5}\right)\left(1+e^{\alpha_1 x-5}\right)}\left(y \le \frac{l_y}{2}\right), \quad (5)$$

$$\kappa_z = \begin{cases} \kappa_{\max}-\kappa_{\min}, & z, \text{atcolapse}, \\ \dfrac{\kappa_{\max}-\kappa_{\min}}{1+e^{(z-Z_c)}-10}, & z, \text{atfracture}, \end{cases} \quad (6)$$

where $\alpha_1 = (10/x_0)$, x_0 is the strike compaction boundary (preset at 70 m); $\alpha_2 = (10/y_0)$, y_0 is the inclination compaction boundary (preset at 20 m); l_y is the workface incline length; $k_{\min}$ is the porosity of crushed rock mass after compaction, ranging from 0.1~0.17 [19]; $k_{\max}$ is the maximum porosity at the workface, which could be obtained by measurement and is commonly ranged from 0.31~0.4 [22].

Substituting equations (5) and (6) into the Kozeny–Carman function [23], one can obtain the goaf permeability distribution [24]:

$$\partial = \frac{{D_p}^2}{180}\cdot\frac{k^3}{(1-k)^2}, \quad (7)$$

where ∂ is permeability at maximum porosity, k is porosity, and D_p is the average particle size, ranging from 0.014 to 0.016 m.

The permeability was compiled with User Defined Functions (UDF) and Renormalization Group (RNG) $k-\varepsilon$ model [25] was adopted to simulate the mixture gas flow in stope considering the turbulence. The distribution of gas in goaf was obtained.

Figure 6 shows the gas concentration distribution in the return airway side section and the goaf plan at different heights. As observed, the gas concentration distributions of the intake and return airways were quite different. The gas concentration of the intake airway was lower, and the low-concentration area was larger than that of the return airway. In the vertical direction, significant stratification of gas was observed near the workface due to air leakage. The closer it

Table 2: Calculation formula parameter value.

Symbol	Parameter	Value	Unit
H	Mining height	5	m
λ	Gas gushing coefficient	1.2	
W_0	Initial gas content of coal seam	11.7	$m^3 \cdot t^{-1}$
W_c	Residual gas content	3.95	$m^3 \cdot t^{-1}$
m	Mining layer thickness	5	m
v_0	Mining velocity of workface	4.1×10^{-3}	$m \cdot min^{-1}$
q_0	Gas gushing intensity of the coal wall	0.0401	$m^3 \cdot (m^2 \cdot min)^{-1}$
l_1	Workface length	185	m
l_1	Strike length of goaf	200	m

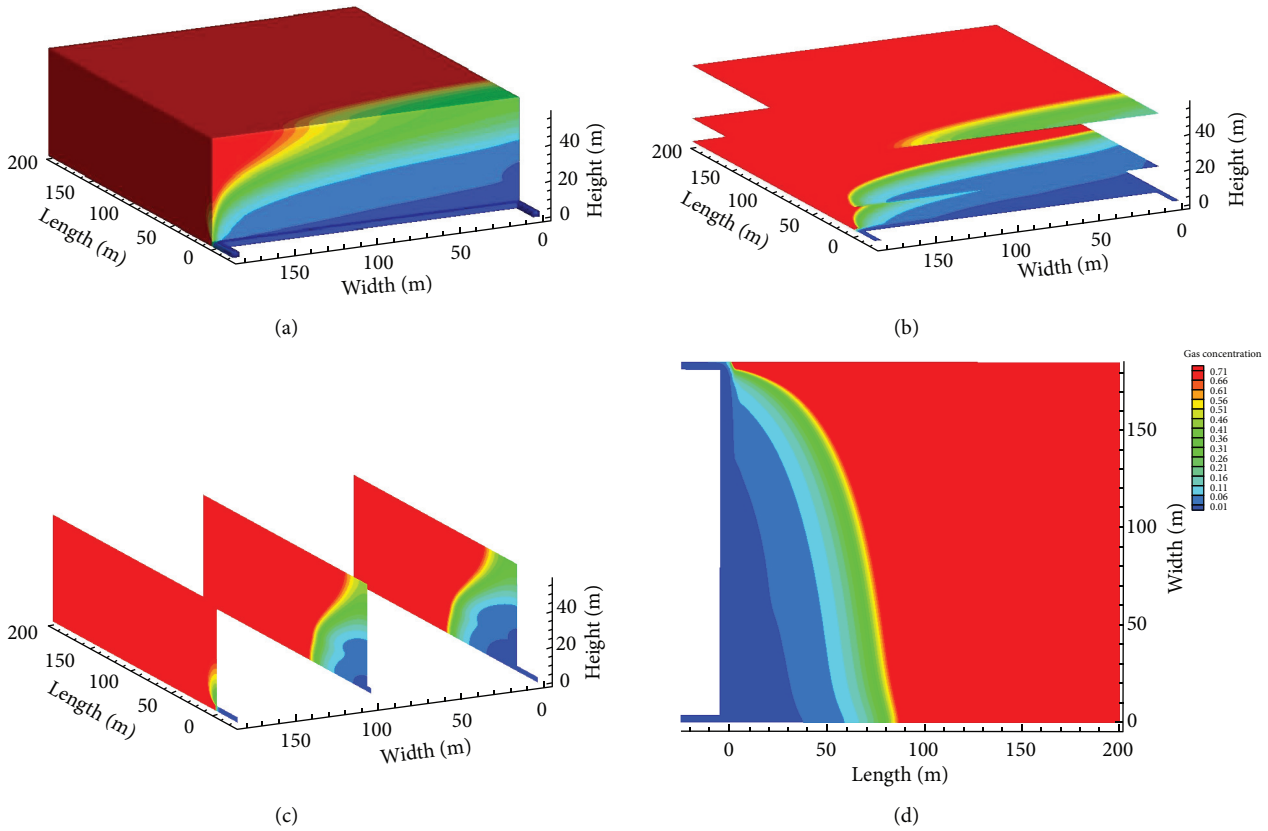

Figure 6: Cloud maps of gas distribution in goaf: (a) 2D scheme; (b) plane map; (c) profile; (d) at a 2 m height.

was to the mining area, the lower the gas concentration was. The upper and deep parts of the goaf were high-concentration gas accumulation areas. Meanwhile, the vortex was developed near the return airway in the workface under the action of negative pressure and coal wall, and the airflow velocity decreased, resulting in gas accumulation and overrun, jeopardizing production safety. The specific distribution was as follows.

Along the strike direction of goaf, the gas concentration in the intake airway was nearly zero due to the influence of fresh airflow. However, the amount of fresh air entering the goaf decreased with the deepening of goaf, and the gas concentration grew from 1 to 60%. The gas concentration near the workface on the return air side was no less than 6%, with a large gradient and high concentration. In the vertical direction, the gas concentration in the return airway was high, with up to 30% being concentrated in the range of 0–30 m in the vertical height and 0–20 m behind the workface.

With no countermeasures, the gas in goaf would get into the return airway under air leakage in the workface. At the same time, due to the action of negative pressure and coal wall, the vortex develops near the upper corner, resulting in the gas overrun in the upper corner, jeopardizing production safety in goaf under HLBs.

For the optimal extraction position obtained above, i.e., 15–45 m in the vertical direction, with the respective support of coal wall and overburden pressure, the optimal position in the horizontal direction can be determined as follows [26]:

$$S = h\cos(\alpha - \beta) + \frac{\gamma(L - L_b)}{2}, \quad (8)$$

where α is the collapse angle of fault zone on the return airway side, set at 85°; β is the dip angle of the coal seam, set at 0°; L is the advancing distance of the workface, set at 200 m; γ is the modification coefficient, set at 1. The compaction area width was preset at 20 m, while a 21.3 m horizontal distance from the return airway was adopted.

The borehole type of the roof's HLB diameter extraction was defined as "Velocity-in," the velocity was $-5\ \mathrm{m{\cdot}s^{-1}}$, and the diameter was 203 mm.

Figure 7 shows the gas concentration distribution of goaf for the HLB (borehole) located 15 m from the floor and 21.3 m from the return airway. As observed, the HLB played a key role in gas drainage in the goaf; the gas in the goaf was discharged by the negative pressure of the HLB and the ventilation airflow. The HLB presence changed the gas flow field at the return air side and the fracture zone. The gas converged to the HLB. The gas concentration at the return air side was lower than that without extraction.

Cloud diagrams of the plane distribution of gas concentration in the goaf, as shown in Figure 8, indicate that the gas concentration in the upper corner decreased to 4% (which was significantly lower than that without extraction), while the low-concentration area at the return air side increased. A negative pressure zone was developed between the gas near the extraction port and the fracture zone, which forced the high-concentration (up to 30%) gas extraction from the fracture zone.

To further study the HLB location effect on the gas distribution in goaf, the gas concentration distribution and extraction volume with the HLBs in different positions were simulated. The preset HLB distances from the floor were 20, 30, and 40 m, respectively, and those from the return airway were 25, 30, and 35, respectively. The results are listed in Table 3.

As observed in Table 3, the optimal extraction parameter corresponded to the borehole located 30 m from the roof and 25 m from the return airway. At this HLB location, the high-concentration gas in the fracture zone could be extracted without affecting the original ventilation airflow. The gas concentration at the upper corner was significantly reduced, and the extraction concentration reached the maximum value. However, simulation results implied that a single borehole could not control the gas concentration at the upper corner within the safe range (>1%).

According to the data in Table 4, the relationship between the HLB parameters and the gas concentration in the drainage pipeline and the gas concentration in the upper corner is obtained through data fitting.

The relationship between the HLB and the gas concentration of the drainage pipeline [27]:

$$W_c = 20.6 + 1.12x + 0.00086xh^2 - 0.0163h^2 - 0.00101h^2. \quad (9)$$

The relationship between the HLB and upper corner gas concentration:

$$W_u = 6.95 + 0.03h + 0.0045x^2 - 0.275x, \quad (10)$$

where W_c is the gas concentration in the drainage borehole, W_u is the gas concentration in the upper corner, x is the distance from the return air tunnel, and h is the height from the floor.

Hence, the number of boreholes should be increased to the number determined by the following equation:

$$N = \frac{4K(Q_J - Q_f)}{VC\pi D^2}, \quad (11)$$

where Q_j and Q_f are the absolute gas emissions of the workface and air row, respectively, K is the disbalance coefficient ranging between 1.2 and 1.7[6], V is the gas flow rate in the sealed pipe, and C is the gas volume fraction in the extraction pipe (%). The actual values of the respective parameters were substituted into equation (11), yielding the required number of boreholes $N = 3$.

According to observation Figures 9 and 10, gas in the fracture zone was accumulated in the borehole under the negative pressure of the borehole; a large amount of high-concentration gas was extracted, and as the high-concentration gas in the goaf moved to the deep part of the goaf as a whole, the gas emission amount was reduced. The gas concentration slice of $Z = 2$ m in the goaf showed that the gas brought out by the airflow entering the goaf was reduced; the upper corner gas concentration was less than 1%, the production safety was ensured, and the safe comining of coal and gas could be realized.

5. Analysis of Drilling and Extraction Effect in Roof Strike

5.1. HLB Application Site Design. According to the simulation results, three directional HLBs were drilled in the roof of workface # 2–104 of the Detong Mine; the drilling yard was located at the paralleled return airway (see Table 4 and Figure 11).

After the completion of drilling construction, continuous observation was performed on the variation of parameters in the process of the workface advance to 200 m, the variation laws of gas concentration in the upper corner and HLB, and the extraction volume with the advance of workface during mining.

5.2. Field Application Analysis. As observed in Figure 12, the variation of gas concentration in the HLB borehole could be subdivided into three stages. In the first stage, the workface advanced by 20 m in the initial mining; fissures above the goaf were rarely developed, and there was no gas concentration area in the goaf. In this case, the gas concentration and net gas extraction amount were almost zero. In the second stage, the workface advanced by 30–75 m; the goaf roof began to collapse under the overburden pressure, the "three-zone" of goaf began to emerge, and the fractures in the fracture zone formed a gas migration channel. At this stage, the gas concentration and volume in the boreholes increased. In particular, gas concentrations in the three

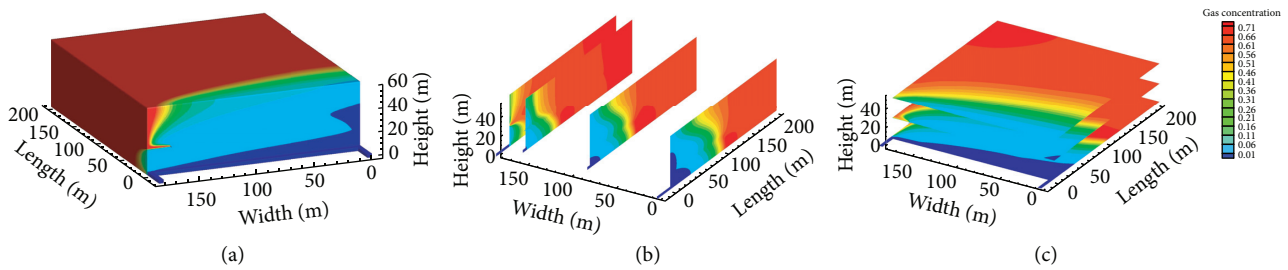

Figure 7: Cloud maps of gas concentration distribution during goaf drainage: (a) in 2D model; (b) in the vertical direction (dip); (c) in the longitudinal (strike) direction.

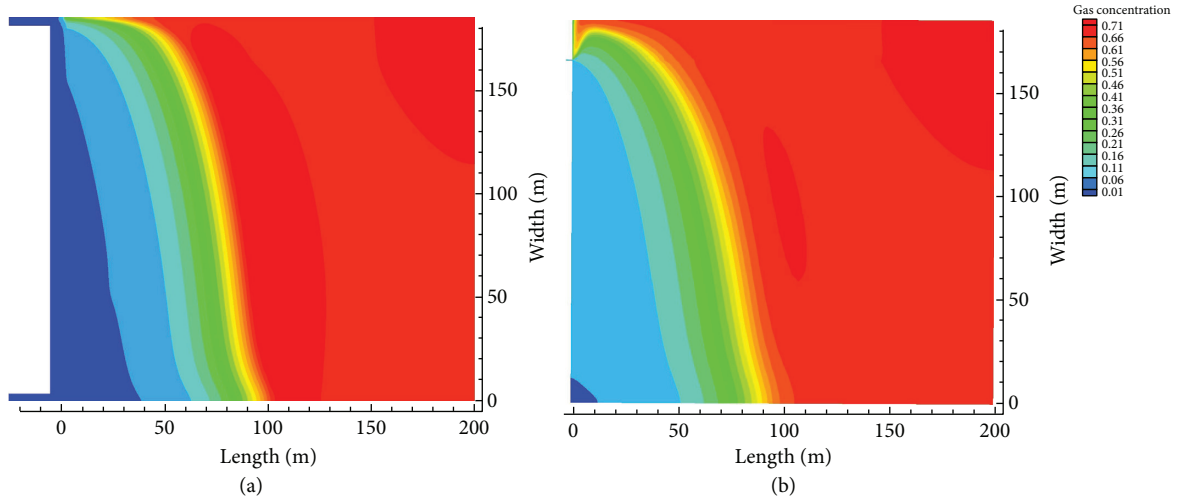

Figure 8: Cloud diagrams of the plane distribution of gas concentration in the goaf: (a) 2 m from the floor; (b) 15 m from the floor.

Table 3: Gas concentrations at nine different HLB locations.

HLB location		Gas concentration, % at the extraction port in the upper corner	
Distance from the roof, m	Distance from the return airway, m		
20	25	33.5	4
20	35	30.3	4.3
20	45	26.8	4.6
30	25	37.5	3.4
30	35	34.5	3.8
30	45	32.8	4.1
40	25	36.4	3.9
40	35	31.5	4.2
40	45	29.5	4.5

Table 4: Construction parameters of roof HLBs.

Hole	Drilling depth/m	Drilling diameter/mm	The horizontal distance between the final hole and roadway/m	The vertical distance between the final hole to the roof/m
1	763	203	30	30
2	782	203	25	30
3	800	203	20	30

boreholes exceeded 35%, and the gas extraction volume was 10 $m^3 \cdot min^{-3}$. At the third stage, when the workface was advanced to 75 m, the fracture zone above the goaf remained stable and shifted with the advancement of the workface. The residual coal and gas desorbed by the coal wall in the goaf continued to accumulate in the goaf, resulting in gas

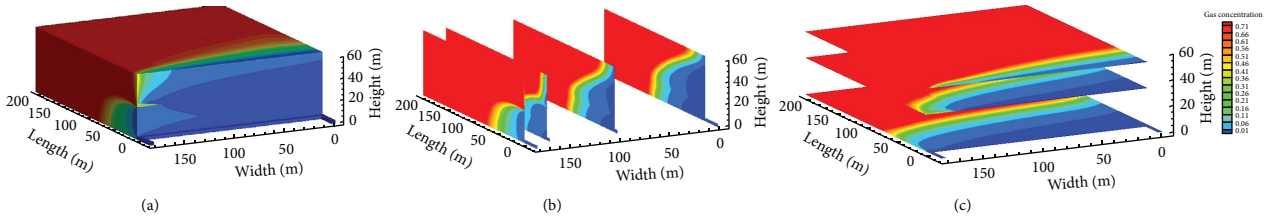

Figure 9: Gas concentration distribution in goaf during drainage of three boreholes: (a) vertical; (b) longitudinal.

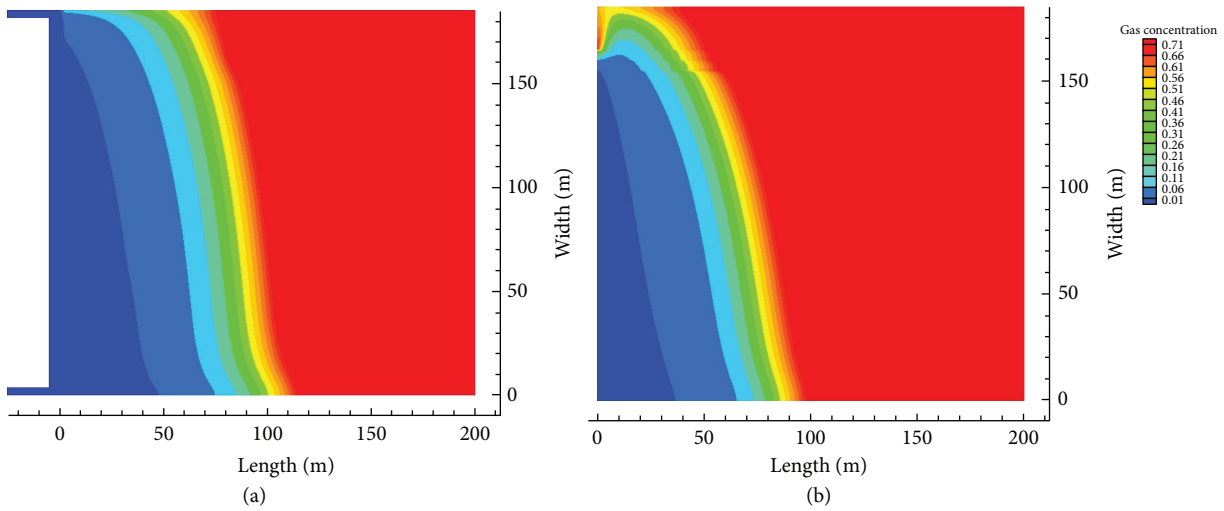

Figure 10: Plane distribution cloud diagram of gas concentration in goaf during drainage of three boreholes: (a) 2 m from the floor; (b) 15 from the floor.

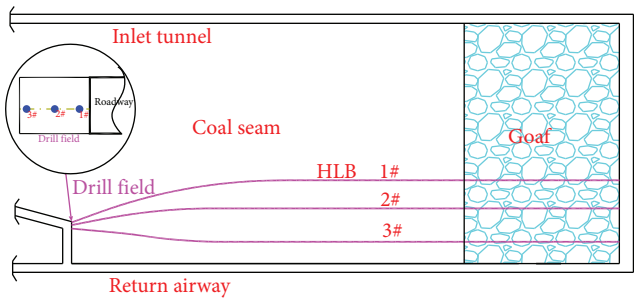

Figure 11: HLB construction diagram.

concentration areas in the deep part of the goaf. Then, the gas floated up to the fracture zone, and the gas concentration in the borehole had a stable and high level. Additionally, a periodic pressure variation of goaf was observed; the gas concentration of the three boreholes was 30–38%, and the gas extraction volume was maintained at 12 $m^3 \cdot min^{-3}$.

In the first and second stages, gas concentration in the upper corner was consistent with the gas extraction volume of the borehole. In a rising trend, the maximum gas concentration in the upper corner reached 0.8%. In the third stage, when the gas concentration and gas extraction volume in the borehole reached a high level, the gas concentration at the upper corner was relatively low, and vice versa. The gas concentration in the upper corner was maintained within the safe range of 0.5–0.6%, and roof HLB parameters obtained by the numerical simulation were quite reliable.

Comparing the actual results on site with the numerical simulation results, the changes in borehole concentration and the upper corner gas concentration were basically consistent with the simulation results. The actual field data is

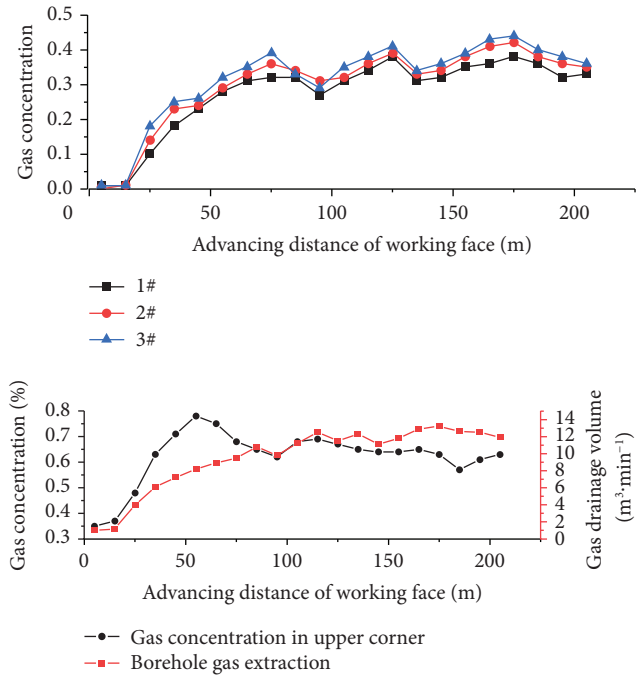

Figure 12: Dynamic change of gas in drainage borehole and upper corner with the movement of working face.

higher than the simulation result. In the following research, the numerical model should be further optimized to avoid errors.

6. Conclusions

Coal mining induces deformation and damage of goaf overburden, resulting in many secondary fractures and gas concentration areas. The gushing of high-concentration gas seriously restricts mining production safety. Therefore, the roof-drilled highly located boreholes (HLBs) are constructed to create an artificial channel to drain the high-concentration gas stored in the fracture zone and improve the production safety with coal and gas comining. Theoretical analysis and FLAC^{3D} numerical simulation were applied to the case study of workface #2-104 of the Detong Mine (China), yielding the goaf overburden stress evolution pattern. Through analysis, it was found that the range of goaf collapse zone was located 15 m from the floor, and the range of fracture zone was 15–60 m from the floor. By defining the pressure relief coefficient, the optimal extraction range of the fracture zone was assessed as 15–45 m; the effective pressure relief angles were 76° in the strike and 85° in the dip. FLUENT software was used to provide the numerical simulation of gas migration law in goaf under initial and different extraction parameters. The results showed that the optimal position of roof-drilled HLB was 30 m from the floor and 25 m from the return airway. It was verified that the problem of the upper corner gas overrun could be mitigated by drilling three directional HLBs. Engineering practice revealed that when three roof-drilled HLBs were located 30 m from the workface floor and 25 m from the return airway, the gas concentration in the boreholes exceeded 30%, while the gas concentration in the upper corner did not exceed 0.8%. The accuracy of the simulation results was verified, which provided a reference for solving gas overrun problems in similar coal mines and realizing effective coal and gas comining.

Data Availability

The data that support the findings of this study are available from the corresponding author upon reasonable request.

Conflicts of Interest

The authors declare that they have no conflicts of interest.

References

[1] Y. Peng, Q. Qi, Y. Wang, Z. Deng, H. Li, and C. Li, "Study of field measurement of mining-induced coal fracture field and its application," *Chinese Journal of Rock Mechanics and Engineering*, vol. 29, no. S2, pp. 4188–4193, 2010.

[2] C. Karacan, G. Esterhuizen, S. Schatzel, and W. P. Diamond, "Reservoir simulation-based modeling for characterizing longwall methane emissions and gob gas vent hole production," *International Journal of Coal Geology*, vol. 71, no. 2-3, pp. 225–245, 2007.

[3] C. Li, Y. Zhang, J. Li, and G. Zhang, "Highly located boreholes drainage technology of gas macroscopic flow channel in goaf," *Journal of Mining & Safety Engineering*, vol. 34, no. 2, p. 7, 2017.

[4] X.-Q. Fang, Y.-Q. Geng, and M. Wang, "Kilometer directional drilling: simultaneous extraction of coal and gas from a high-gas coal seam," *Journal of China University of Mining and Technology*, vol. 41, no. 6, pp. 885–892, 2012.

[5] Y. P. Cheng, Q.-X. Yu, L. Yuan, and P. Li, "Experimental research of safe and high-efficient exploitation of coal and pressure relief gas in long-distance," *Journal of China*

University of Mining and Technology, vol. 33, no. 2, pp. 132–136, 2004.

[6] M. G. Qian and J. L. Xu, "Study on the "O shape" circle distribution characteristics of mining induced fracture in the overburden strata," *Journal of China Coal Industry*, vol. 5, pp. 20–23, 1998.

[7] H. Yavuz, "An estimation method for cover pressure re-establishment distance and pressure distribution in the goaf of longwall coal mines," *International Journal of Rock Mechanics and Mining Sciences*, vol. 41, no. 2, pp. 193–205, 2004.

[8] C. Ö. Karacan and R. M. Goodman, "Hydraulic conductivity changes and influencing factors in overburden determined by slug tests in gob gas ventholes," *International Journal of Rock Mechanics and Mining Sciences*, vol. 46, no. 7, pp. 1162–1174, 2009.

[9] H. Guo, L. Yuan, B. Shen, Q. Qu, and J. Xue, "Mining-induced strata stress changes, fractures and gas flow dynamics in multi-seam longwall mining," *International Journal of Rock Mechanics and Mining Sciences*, vol. 54, pp. 129–139, 2012.

[10] S. Li, H. Lin, P. Zhao, P. Xiao, and H. Pan, "Dynamic evolution of mining fissure elliptic paraboloid zone and extraction coal and gas," *Journal of China Coal Society*, vol. 39, no. 8, pp. 1455–1462, 2014.

[11] V. Palchik, "Formation of fractured zones in overburden due to longwall mining," *Environmental Geology*, vol. 44, no. 1, pp. 28–38, 2003.

[12] M. Qin, "Study on the treatment of upper corner gas based on the roof-drilling holes," *Innovation and Application of Engineering Technology*, CRC Press, Florida, USA, 2017.

[13] G. Si, S. Jamnikar, J. Lazar et al., "Monitoring and modelling of gas dynamics in multi-level longwall top coal caving of ultra-thick coal seams, part I: borehole measurements and a conceptual model for gas emission zones," *International Journal of Coal Geology*, vol. 144-145, pp. 98–110, 2015.

[14] Q. Bai, S. Tu, Y. Yuan, and F. Wang, "Back analysis of mining induced responses on the basis of goaf compaction theory," *Zhongguo Kuangye Daxue Xuebao/Journal of China University of Mining and Technology*, vol. 42, no. 3, pp. 355–361, 2013.

[15] Z. Meng, J. Zhang, X. Shi, Y. Tian, and Y. Chao, "Calculation model of rock mass permeability in coal mine goaf and its numerical simulation analysis," *Journal of China Coal Society*, vol. 41, no. 8, pp. 1997–2005, 2016.

[16] L. Yuan, H. Guo, B.-T. Shen, Q.-D. Qu, and X. Junhua, "Circular overlying zone at longwall panel for efficient methane capture of multiple coal seams with low permeability," *Journal of China Coal Society*, vol. 36, no. 3, p. 365, 2011.

[17] J. Ma, Y. Sun, and B. Li, "Simulation of combined conductive, convective and radiative heat transfer in moving irregular porous fins by spectral element method," *International Journal of Thermal Sciences*, vol. 118, pp. 475–487, 2017.

[18] Z. Qin, L. Yuan, H. Guo, and Q. Qu, "Investigation of longwall goaf gas flows and borehole drainage performance by CFD simulation," *International Journal of Coal Geology*, vol. 150-151, pp. 51–63, 2015.

[19] H. Zhao, W. Pan, and X. Wang, "Numerical simulation on distribution of gas concentration in goaf under condition of mining thin coal seam," *Journal of China Coal Society*, vol. 36, pp. 440–443, 2011.

[20] W. Wang, Z. Li, and H. Yu, "Goaf Gas control improvement by optimizing the adjacent roadway large-diameter boreholes," *Advances in Civil Engineering*, vol. 2021, Article ID 1933010, 13 pages, 2021.

[21] W. Wei, Y. Cheng, H. Liu, Z. Fang, X. Li, and R. Zhao, "Permeability model of gob based on sigmoid function and application in the airflow field simulation," *Journal of Mining & Safety Engineering*, vol. 34, no. 6, p. 1232, 2017.

[22] Z.-X. Li, S.-L. Ji, and Z.-Y. Ti, "Two-phase miscible diffusion model and its solution between gas in goaf and atmosphere," *Chinese Journal of Rock Mechanics and Engineering*, vol. 24, no. 16, pp. 2971–2976, 2005.

[23] B. Tan, J. Shen, D. Zuo, and X. Guo, "Numerical analysis of oxidation zone variation in goaf," *Procedia Engineering*, vol. 26, pp. 659–664, 2011.

[24] G. Wang, H. Xu, M. Wu, Y. Wang, R. Wang, and X. Zhang, "Porosity model and air leakage flow field simulation of goaf based on DEM-CFD," *Arabian Journal of Geoences*, vol. 11, no. 7, pp. 1–17, 2018.

[25] V. Yakhot, S. A. Orszag, S. Thangam, T. B. Gatski, and C. G. Speziale, "Development of turbulence models for shear flows by a double expansion technique," *Physics of Fluids A: Fluid Dynamics*, vol. 4, no. 7, pp. 1510–1520, 1992.

[26] S.-G. Li, P.-Y. Xu, P. Zhao, and H. Lin, "Aging induced effect of elliptic paraboloid zone in mining cracks and pressure released gas drainage technique," *Coal Science and Technology*, vol. 46, no. 9, pp. 146–152, 2018.

[27] B. Zhao, G. Wen, J. Nian et al., "Numerical simulation study on the multi-physical field response to underground coal and gas outburst under high geo-stress conditions," *Minerals*, vol. 12, no. 2, Article ID 151, 2022.